Acta Med. Okayama, 2022
Vol. 76, No. 5, pp. 565-575

Acta Medica Okayama
http://escholarship.lib.okayama-u.ac.jp/amo/

Original Article

A Simple and Descriptive Assessment of Morphology Based on the Horizontal Plane of the Pediatric Head and Creation of a Normative Database in Japanese Children 6 Years Old and under: Horizontal Vector Analysis

Sho Komagoe[a]*, Takaya Senoo[a], Soshi Takao[b], Yoshinori Shiraishi[a], Hiroshi Matsumoto[a], and Yoshihiro Kimata[a]

Departments of [a]Plastic and Reconstructive Surgery, [b]Epidemiology, Okayama University Graduate School of Medicine, Dentistry and Pharmaceutical Sciences, Okayama 700-8558, Japan

We herein introduce horizontal vector analysis, a simple method for assessing cranial morphology based on measurement of the head's horizontal plane, and use this method to establish normal cranial morphology in Japanese children Computed tomography scans taken in 2010-2019 in healthy Japanese children aged ≤6 years. The two measurement planes were parallel to the orbitomeatal plane: namely, a plane passing through the dorsum sellae (DS) and the plane superior to that with the maximal area (Max plane). A protractor was used to circumferentially measure the lengths from the central point to the outer surface of the skull. A total of 487 images were extracted. The distances between the DS and Max planes were consistently almost 30 mm for each age group, so we fixed the Max plane as the plane 30 mm superior to the DS plane. Finally, we established datasets of normal values for each age group and sex. Using these norms, perioperative evaluation of various cranial deformities could be performed more easily and circumstantially.

Key words: craniofacial surgery, craniosynostoses, horizontal plane, Japanese children, reference values

Surgical treatment is often performed in children with craniosynostosis if their brain growth is at risk of being stunted or cosmetic deformities are remarkable. However, there are no standard perioperative measurement methods or normal values for the assessment of cranial morphology in healthy Japanese children.

The cephalic index is a widely used parameter that describes the ratio of the maximum width of the head to the maximum occipitofrontal length. Despite several reports on normal cephalic index values [1-3], this index does not characterize the cranial morphology in sufficient detail to be useful in most cases.

Three-dimensional photogrammetric techniques, such as 3dMDface System® (3dMD, Atlanta, CA, USA), and eye-safe laser surface scanning, such as STARscanner® (Orthomerica, Orlando, FL, USA), are increasingly being used for the morphological evaluation of cranial deformities [4-7]. As these are rapid, easy-to-apply, and non-invasive methods, they are very useful for pre and postoperative evaluations of the silhouettes of patients' heads. Nonetheless, it is difficult to apply the collected images and data to detailed preoperative planning. They are not beneficial for making decisions regarding the amount and directions of movements of skull bones.

Some studies have performed three-dimensional measurement of cranial morphology using dedicated

Received January 14, 2022; accepted May 2, 2022.
*Corresponding author. Phone: +81-86-235-7214; Fax: +81-86-235-7210
E-mail: sho.komagoe@gmail.com (S. Komagoe)

Conflict of Interest Disclosures: No potential conflict of interest relevant to this article was reported.

software and workstations [8-11] and have recorded normal values using these devices [12-14]; however, the devices are expensive, so these methods have also shown a lack of versatility.

Prior to the emergence of these three-dimensional measurement methods [8], Marcus *et al.* introduced a simplified method for measuring detailed cranial morphology on the midsagittal plane using midsagittal vector analysis (MSVA) [15]. MSVA is a radial vector analysis that uses a full circular protractor on the midsagittal plane, and the distances from the summit of the dorsum sellae (DS) to the outer surface of the skull are presented in 10° increments (Fig. 1A). The cranial morphology from the lateral view is shown in Fig. 1B. Senoo *et al.* used MSVA to determine the normal cranial values for different age groups of Japanese children [16].

Very few studies have reported in detail the simplified normal cranial morphology of Japanese children [16, 17]; thus, it is necessary to determine the normal values on planes other than the midsagittal plane to broaden the field of application.

The horizontal or axial plane of the head is frequently used in clinical practice; indeed, the traditional measurement of head circumference assesses this plane. Therefore, this study aimed to introduce horizontal vector analysis (HoVA), which is a simplified and detailed cranial measurement method based on the horizontal plane, and to establish the normal HoVA values for Japanese children of different ages.

Materials and Methods

Patient selection. We extracted head computed tomography (CT) scans of patients aged 0-83 months taken at Okayama University Hospital between January 2010 and December 2019. Patients were classified into nine age groups: 0M, 0-2 months; 3M, 3-5 months; 6M, 6-11 months; 1Y, 12-23 months; 2Y, 24-35 months; 3Y, 36-47 months; 4Y, 48-59 months; 5Y, 60-71 months; 6Y, 72-83 months. We selected the age groups with reference to previous studies that have reported on the normal cranial morphology of children using the midsagittal plane [16] and three-dimensional images [12].

We retrospectively reviewed the electronic charts of all cases and set the following exclusion criteria: height and weight ≤ -2 or >2 standard deviations [SD] in the Japanese standard growth curve, low birth weight ($<2{,}500$ g), hydrocephalus, intracranial mass, craniosynostosis, huge subarachnoid cyst, including fracture or skull defect at the measurement site, intractable epilepsy (requiring permanent medication), developmental disorder (with developmental quotient <70 in the Kyoto Scale of Psychological Development 2001), long-term chemotherapy, chromosomal abnormality, and hypothyroidism. Similarly, we excluded cases with highly blurred images or cases wherein the imaging

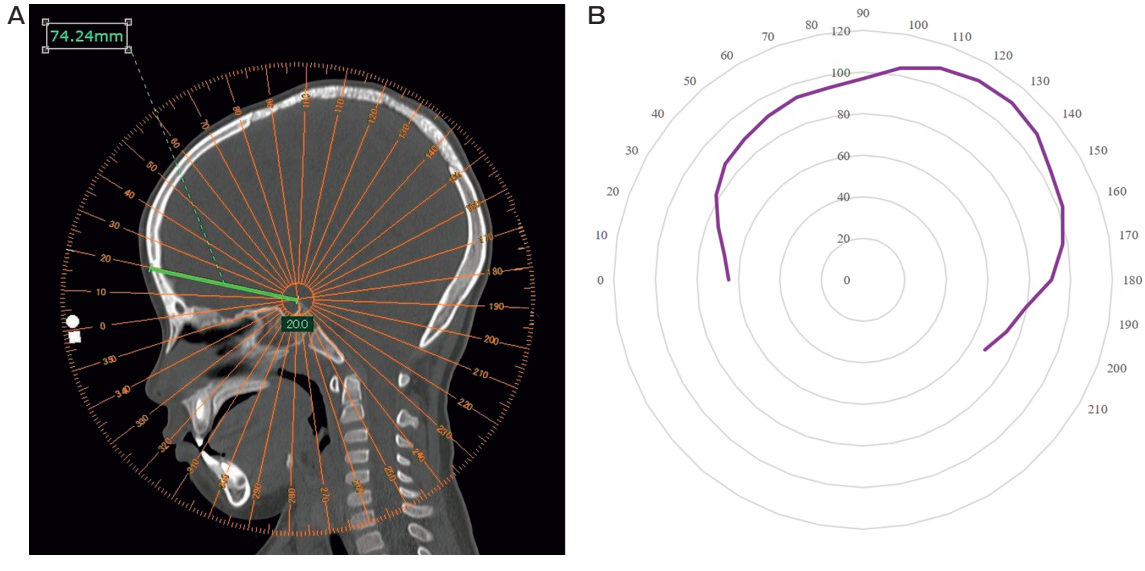

Fig. 1 Midsagittal vector analysis. (A) The measurement is performed on the screen. (B) The measurement result reveals the cranial morphology from the lateral view.

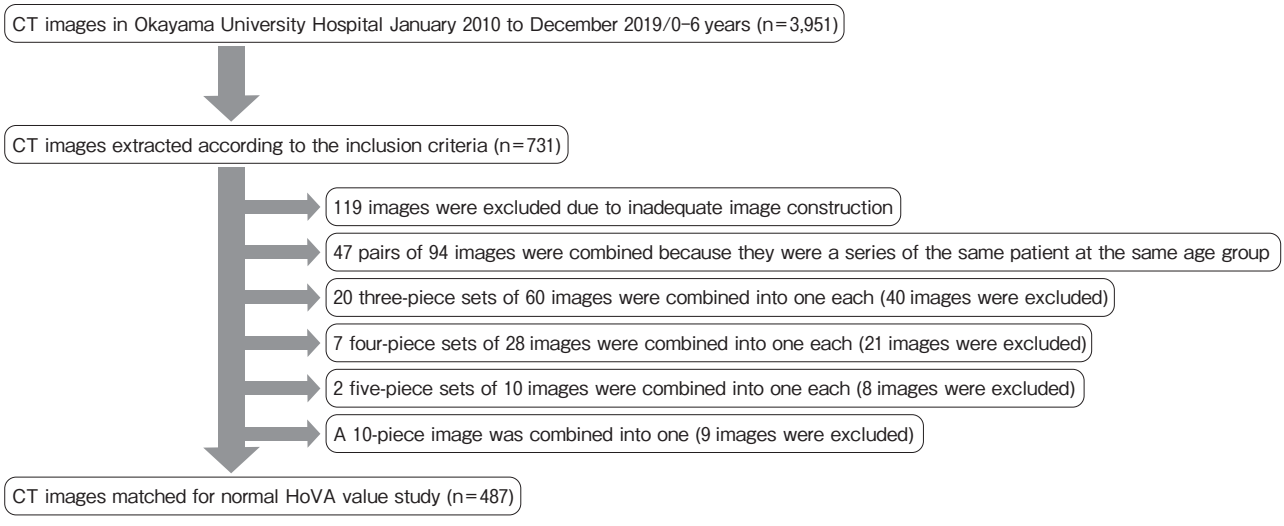

Fig. 2 Subject flow chart. CT, computed tomography; HoVA, horizontal vector analysis.

Table 1 Characteristics of the study population

Age group	Female	Male	Total
0M	20	22	42
3M	15	21	36
6M	31	26	57
1Y	51	57	108
2Y	28	26	54
3Y	27	17	44
4Y	19	29	48
5Y	24	28	52
6Y	21	25	46
Total	236	251	487

0M, 0–2 months; 3M, 3–5 months; 6M, 6–11 months; 1Y, 12–23 months; 2Y, 24–35 months; 3Y, 36–47 months; 4Y, 48–59 months; 5Y, 60–71 months; 6Y, 72–83 months.

Table 2 Reason for examination

Acute inflammation	54
Seizure or epilepsy	33
S/O cranial dysplasia	58
Trauma	124
Hematologic disease (early screening after onset)	39
H&N tumor (early screening after onset when malignancy was diagnosed)	26
Intracranial hemorrhage or vascular lesion	18
Cephalic or subcutaneous hematoma	6
Screening for latent spina bifida or spinal lipoma	16
Screening for neuromuscular disease	5
SIDS or CPAOA	11
Drowning	8
S/O intracranial tumor or brain metastasis	22
S/O intracranial lesion associated with congenital disease	15
Head and neck pain	12
S/O growth or developmental disorder	9
Whole body screening for benign lesion	9
Others	22
Total	487

S/O, suspected of; H&N, head and neck; SIDS, sudden infant death syndrome; CPAOA, cardiopulmonary arrest on arrival.

ranges were insufficient for measurement. We included diseases such as acute encephalopathy and small dermoid cyst because in our opinions they were not affecting cranial growth at the time of the CT. We averaged all measurement values for cases in which CT was performed several times while the patient was the same age.

We collected 3,951 head CT images, from which we extracted 731 images after excluding patients with characteristics affecting cranial growth. Similarly, we excluded insufficiently constructed images (n=119) and optimized overlapping samples (47×2, 20×3, 7×4, 2×5, and 1×10 images were combined). Finally, we analyzed 487 images (251 male and 236 female). Figure 2 presents the study participant flowchart. Tables 1 and 2 present the characteristics of the study population and reasons for examination, respectively.

This study was conducted in accordance with the principles embodied in the Declaration of Helsinki and was approved by the ethics committee of the Okayama University Hospital (research no. 2002-008). Informed consent was obtained using the opt-out method on the hospital website. We adhered to the STARD guidelines.

Determination of the measuring method and validation of the method. To determine and validate the measurement method, we only used a small number of subsets out of a total of 487 cases: 45 cases (all age categories) for determining the distance between the first and second measurement planes, 5 cases (0M and 6M female; 3M, 1Y, and 3Y male) for estimating the inter-rater reliability, and 5 cases (0M, 3M, and 6M female; 1Y and 5Y male) for evaluating the difference caused by the tilt of the plane. Statistical calculations were performed using SPSS version 25.0 (IBM Corp., Armonk, NY, USA).

We used two CT scan slices parallel to the orbitomeatal (OM) plane for the measurement because the OM plane is the most common horizontal plane of the head. When slices were not constructed parallel to the OM plane, we used AZE Virtual Place® (AZE, Tokyo) for reconstruction. The measurement was performed using SYNAPSE VINCENT® (Fujifilm, Tokyo) and a digital protractor (protractor. exe; Daigo, https://www.vector.co.jp/soft/winnt/util/se345469.html).

Determination of the first/second measurement plane. We determined the plane passing through the summit of the DS as one of the measurement planes (Fig. 3, lower left), which we termed the "DS plane." Another measurement plane superior to the DS plane was established because the range of clinical applications for craniofacial surgery is restricted when using the DS plane only. We used the plane with a maximal cranial area, which we termed the "Max plane" (Fig 3, upper left). Although this plane could be hand-selected for each case, to do so would require considerable effort. Thus, to ensure clinical usefulness, we decided to fix the distance between these two planes. One cross-section in one patient from the 45 cases was arbitrarily selected and the area was measured 20 times to verify the reliability of manual measurement (Fig. 4). The mean (95% confidence interval [lower limit-upper limit]) for the area was 18,816.6 (18,805.8-18,827.3) mm^2; hence, the width of the confidence interval was 21. 5 (*i.e.*, = 18,827.3-18,805.8). This width was small, so we considered the measurement to be reliable. Subsequently, we decided the maximal cranial area in all 45 cases. The distances for each age group were plotted in the scatter diagram, and an approximation straight line was fitted. Finally, we fixed the distance and the two measurement planes.

Inter-rater reliability. The center of the digital protractor was placed at the center of the summit of the DS, and the 0° line was set at the nasofrontal suture. The lengths from the central surface to the skull surface were measured from 0° to 180° in 10° increments. We recorded the average of the left and right values from 10° to 170°. After measuring the distances on the DS plane, images were scrolled up to the Max plane, with the protractor fixed; subsequently, the lengths from the central surface to the skull surface were measured circumferentially, as performed on the DS plane (Fig. 3).

Three trained readers independently measured the DS and Max planes seven times in the above-men-

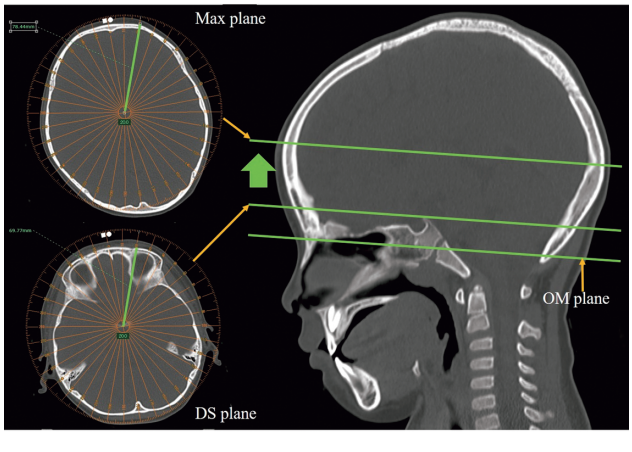

Fig. 3 The orbitomeatal (OM), dorsum sellae (DS), and maximal cranial area (Max) planes. The DS plane is the plane passing through the summit of the DS, and the Max plane is the plane with the maximal cranial area.

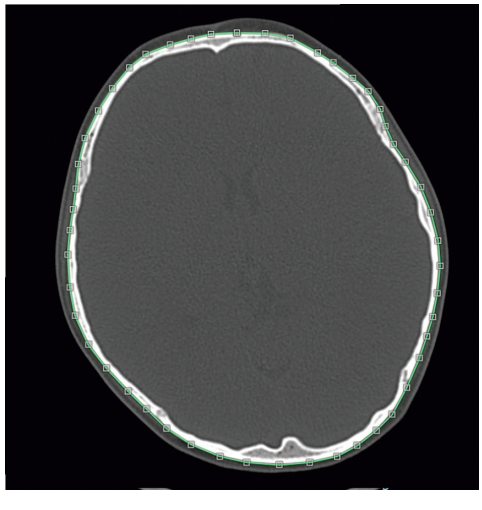

Fig. 4 Measurement of cranial areas. The area was measured 20 times to verify the reliability of manual measurement.

tioned 5 cases, for a total of 21 measurements each for the DS and Max planes in these cases. We thought that the verification of the measurements via typical statistical approaches would be difficult; thus, we used the following methods.

First, the lengths at 0° in the 5 cases were measured seven times by reader A; *i.e.*, reader A measured the lengths at 0° a total of 35 times. Subsequently, we calculated the Pearson correlation coefficient between all 35 lengths at 0° measured by reader A and those measured by reader B. The correlation coefficients from 10° to 180° were also calculated similarly between readers A and B. Furthermore, we conducted the same calculation between readers B and C and between readers A and C.

Next, we calculated the Pearson correlation coefficient between lengths from 0° to 180° measured by reader A and those measured by reader B in a 0M female patient. The correlation coefficient between readers B and C and between readers A and C were calculated in the same manner for this patient. We performed the same calculation for the remaining 4 cases.

Lastly, we compared the between-readers and within-reader errors using analysis of variance (ANOVA).

Effect of the tilt of the OM plane on measurement error. The OM plane is defined as the plane passing through both the external auditory openings and the outer canthi of the eyes or the center of the orbits. The center of the orbits is often defined subjectively, and a tilt from the true OM plane can occur in the sagittal plane.

We created the true OM plane (0° plane) passing through both the external auditory openings and the outer canthi of both eyes three-dimensionally. The 0° plane was rotated in 1° increments to ±5° on the mid-sagittal plane using AZE Virtual Place®. We calculated the measurement errors from the 0° plane on each tilted plane. We did not investigate the effect of the tilt of the OM plane on the coronal plane because the definition of the 0° plane is considered difficult due to the variable left-right asymmetry of the human body [11, 18].

Creation of a normative database of HoVA in Japanese children. After determining and validating the measuring method, we performed HoVA for all cases over 487. We then calculated the means and SDs of the measured values for each plane, sex, and age group. Radar charts of each mean HoVA value were created using Microsoft Excel® 2019 (Microsoft, Redmond, WA, USA).

Results

Determination of the Max plane. Figure 5 shows the measurement results of the distance between the DS and Max planes. The distance became slightly decreased at more advanced ages; however, the fitted straight line (red line) passed through approximately 30 mm. Therefore, we fixed the Max plane as the plane 30 mm superior to the DS plane for all age groups.

Inter-rater reliability. Table 3 presents the correlation coefficients at the 36 measurement sites and for each of the 5 cases on the DS and Max planes. The correlation coefficients ranged from approximately 0.898 to 1.000 on both planes. In addition, ANOVA did not reveal significant differences between readers on the DS plane ($F = 0.348$, $p = 0.706$) or the Max plane ($F = 0.427$, $p = 0.653$).

Effect of the tilt of the OM plane on measurement error. Table 4 presents the means of the measurement errors for the 5 cases at each measurement site from 0° to 180° from the 0° plane. We averaged the left and right values from the 10° to 170° sites. Moreover, we calculated the means for every angle between 0° to 180° for each degree of tilt. If the tilt was within ±3°, the means were less than 1.1 mm. However, if the tilt was greater than ±4°, the means ranged from 1.28 to 1.99 mm.

Normal HoVA values in Japanese children. Tables 4-8 present the measurement results of the means and SDs using HoVA. Figure 6 shows the radar

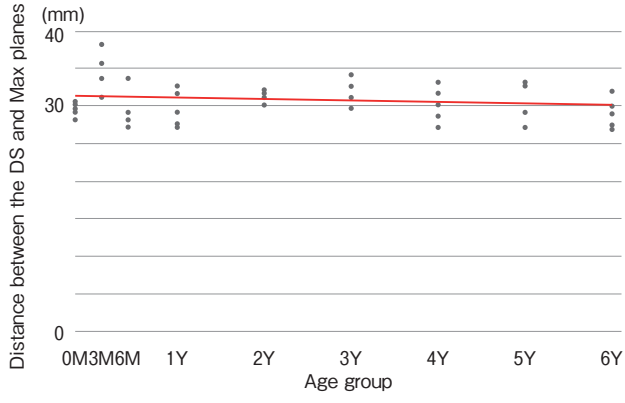

Fig. 5 Distance between the DS and Max planes for each age group. DS plane, dorsum sellae plane; Max plane, plane with the maximal cranial area above the DS plane; 0M, 0–2 months; 3M, 3–5 months; 6M, 6–11 months; 1Y, 12–23 months; 2Y, 24–35 months; 3Y, 36–47 months; 4Y, 48–59 months; 5Y, 60–71 months; 6Y, 72–83 months.

Table 3 Correlation coefficients among three readers (reader A, B, and C)

DS plane [a]	0°	L10°	L20°	L30°	L40°	L50°	L60°	L70°	L80°	L90°	L100°	L110°	L120°	L130°	L140°	L150°	L160°	L170°	L180°
A and B	0.998	0.997	0.997	0.997	0.993	0.966	0.989	0.981	0.987	0.99	0.993	0.993	0.996	0.996	0.993	0.997	0.997	0.998	0.998
B and C	0.997	0.998	0.997	0.998	0.997	0.981	0.996	0.992	0.992	0.993	0.995	0.996	0.997	0.989	0.992	0.996	0.995	0.998	0.997
A and C	0.997	0.996	0.996	0.997	0.992	0.963	0.988	0.978	0.985	0.988	0.993	0.994	0.995	0.988	0.992	0.997	0.996	0.997	0.998

	R10°	R20°	R30°	R40°	R50°	R60°	R70°	R80°	R90°	R100°	R110°	R120°	R130°	R140°	R150°	R160°	R170°
	0.997	0.994	0.995	0.987	0.923	0.963	0.982	0.969	0.977	0.983	0.993	0.996	0.996	0.997	0.998	0.999	0.999
	0.997	0.995	0.995	0.993	0.934	0.966	0.973	0.98	0.991	0.994	0.997	0.998	0.998	0.999	0.999	0.999	0.999
	0.995	0.993	0.994	0.99	0.898	0.929	0.954	0.947	0.975	0.983	0.99	0.996	0.995	0.998	0.998	0.998	0.998

Max plane [b]	0°	L10°	L20°	L30°	L40°	L50°	L60°	L70°	L80°	L90°	L100°	L110°	L120°	L130°	L140°	L150°	L160°	L170°	L180°
A and B	0.996	0.996	0.996	0.995	0.994	0.992	0.991	0.992	0.989	0.991	0.99	0.99	0.986	0.988	0.989	0.996	0.997	0.998	0.998
B and C	0.996	0.997	0.997	0.997	0.997	0.996	0.995	0.995	0.996	0.996	0.996	0.995	0.993	0.991	0.988	0.995	0.996	0.998	0.998
C and A	0.996	0.996	0.995	0.993	0.992	0.989	0.992	0.992	0.991	0.989	0.986	0.99	0.978	0.986	0.99	0.995	0.995	0.997	0.997

	R10°	R20°	R30°	R40°	R50°	R60°	R70°	R80°	R90°	R100°	R110°	R120°	R130°	R140°	R150°	R160°	R170°
	0.995	0.996	0.993	0.989	0.987	0.992	0.992	0.986	0.99	0.994	0.995	0.996	0.997	0.997	0.997	0.998	0.999
	0.994	0.995	0.992	0.99	0.991	0.991	0.995	0.995	0.996	0.998	0.997	0.998	0.998	0.998	0.998	0.998	0.999
	0.994	0.994	0.992	0.991	0.986	0.987	0.989	0.986	0.985	0.993	0.993	0.997	0.997	0.998	0.997	0.998	0.998

DS plane [c]	A and B	B and C	C and A
0M, female	0.979	0.998	0.978
3M, male	0.957	0.988	0.938
6M, female	0.996	0.999	0.997
1Y, male	0.994	0.999	0.993
3Y, male	1.000*	0.999	0.999

Max plane [d]	A and B	B and C	C and A
0M, female	0.99	0.999	0.99
3M, male	0.978	0.993	0.966
6M, female	0.998	0.999	0.999
1Y, male	0.986	0.995	0.978
3Y, male	1.000*	0.999	0.998

DS plane, dorsum sellae plane; Max plane, plane with the maximal cranial area above the DS plane; L, left; R, right; M, months; Y, years. *0.995 or more.
[a] correlation coefficients at the 36 measurement sites on the DS plane. [b] correlation coefficients at the 36 measurement sites on the Max plane.
[c] correlation coefficients for each of the 5 cases on the DS plane. [d] correlation coefficients for each of the 5 cases on the Max plane.

Table 4 Average measurement error of 5 cases at all measurement sites on the DS plane and Max planes

	0°	10°	20°	30°	40°	50°	60°	70°	80°	90°	100°	110°	120°	130°	140°	150°	160°	170°	180°	Mean of 0° to 180°
DS plane (mm)																				
+1°	0.58	0.74	0.69	0.47	0.4	0.64	0.37	0.61	0.54	0.46	0.48	0.55	0.54	0.49	0.46	0.6	0.61	0.69	0.92	0.57
+2°	1.02	1.11	1.07	0.8	0.41	0.89	0.62	0.49	0.47	0.33	0.43	0.57	0.56	0.67	0.75	0.64	0.8	0.97	0.8	0.71
+3°	1.88	2.14	2.04	1.42	0.55	1.25	1.02	0.68	0.48	0.37	0.33	0.61	0.56	0.85	1.15	1.21	1.34	1.58	1.46	1.1
+4°	2.62	3.03	2.76	1.89	0.78	1.66	1.27	1.7	0.53	0.34	0.47	0.69	1.01	1.33	2.09	2.03	1.96	2.12	2.18	1.6
+5°	3.18	3.43	3.15	2.26	0.86	2.09	1.54	0.99	0.65	0.39	0.45	0.86	1.2	1.48	2.32	2.31	2.18	2.51	2.24	1.79
−1°	0.76	0.79	0.99	0.44	0.29	0.55	0.28	0.35	0.43	0.48	0.32	0.57	0.56	0.5	0.69	0.79	0.81	0.87	1.56	0.63
−2°	1.22	1.61	1.72	0.68	0.35	1.09	0.78	0.78	0.69	0.46	0.4	0.57	0.64	0.61	1.08	1.07	1.28	1.39	1.84	0.96
−3°	1.24	1.68	1.61	0.58	0.27	1.16	0.77	0.51	0.52	0.34	0.44	0.72	0.75	0.91	0.96	1.24	1.53	1.75	1.88	0.99
−4°	2.24	2.81	2.39	1.08	0.43	1.57	1.25	0.74	0.63	0.52	0.5	0.85	1.1	1.39	1.39	2.08	2.23	2.94	3.64	1.57
−5°	2.64	3.13	2.63	1.06	0.36	2.01	1.42	0.94	0.67	0.37	3.6	1.13	1.27	1.66	2.05	2.28	2.7	3.52	4.32	1.99
Max plane (mm)																				
+1°	0.48	0.32	0.42	0.36	0.25	0.43	0.38	0.22	0.29	0.24	0.26	0.38	0.36	0.44	0.32	0.48	0.64	0.63	0.38	0.38
+2°	0.46	0.41	0.47	0.33	0.5	0.37	0.47	0.32	0.28	0.22	0.31	0.28	0.39	0.5	0.63	0.72	0.93	1.08	0.68	0.49
+3°	0.82	0.86	0.9	0.64	0.75	0.82	0.79	0.69	0.54	0.41	0.43	0.48	0.71	0.97	1.05	1.33	1.68	1.97	1.58	0.92
+4°	1.36	1.24	1.19	0.95	1.08	1.1	1.03	0.99	0.67	0.46	0.35	0.51	1.1	1.21	1.45	1.94	2.23	3	2.44	1.28
+5°	1.36	1.34	1.19	0.99	1.14	1.19	1.18	1.12	0.85	0.54	0.48	0.64	1.19	1.5	1.73	2.23	2.67	3.54	3	1.47
−1°	0.6	0.45	0.34	0.41	0.35	0.31	0.32	0.35	0.26	0.22	0.33	0.35	0.51	0.48	0.51	0.55	0.54	0.76	0.8	0.44
−2°	1.16	1.06	0.9	0.83	0.84	0.84	0.54	0.56	0.47	0.3	0.3	0.37	0.6	0.84	1.06	1.02	1.25	1.71	1.58	0.85
−3°	1.04	0.94	0.78	0.8	0.79	0.83	0.69	0.81	0.66	0.32	0.29	0.43	0.77	0.97	1.13	1.19	1.36	1.61	1.5	0.89
−4°	1.86	1.68	1.42	1.32	1.32	1.26	0.92	1.1	0.92	0.39	0.37	0.72	1.15	1.49	1.81	1.97	2.09	2.53	2.4	1.41
−5°	2.16	1.94	1.55	1.5	1.59	1.44	1.18	1.32	0.96	0.52	0.77	0.73	1.28	1.81	2.21	2.26	2.48	2.79	2.6	1.64

DS plane, dorsum sellae plane; Max plane, plane with the maximal cranial area above the DS plane.

Table 5 Measurement results of the mean of the DS plane using HoVA

Female	Angle	0°	10°	20°	30°	40°	50°	60°	70°	80°	90°	100°	110°	120°	130°	140°	150°	160°	170°	180°
	0M	46.6	46.6	47	47.6	46.6	43.1	40.2	40.7	40.5	40.4	40.6	41.6	43.5	45.4	46.5	47.8	47.7	47	47
	3M	53.4	53.1	53.5	54.5	53.9	49.4	47.2	48.3	48.7	49.1	49.8	51.4	53.8	55.6	56.9	57.9	57.6	56.3	55.6
	6M	59.5	58.5	58.7	59.4	57.4	51.7	49.3	50.3	50.7	51.3	53	56	59.2	62.2	64.4	66.9	67.3	66.2	65.5
	1Y	64.1	62.8	62.8	63	60.6	54	56.3	52.8	53.6	54.4	56.2	59.3	63.2	66.2	68.6	70.7	71.1	70.3	69.3
	2Y	66.3	65	64.9	65.1	62.5	54.5	52.2	53.9	55.6	57.2	59.4	62.9	67.3	70.6	73.1	75.3	75.9	74.8	73.6
	3Y	67.5	66.3	66.3	66.2	63.9	55.7	52.9	54.5	56.6	58.3	60.4	64	68.9	72.8	75.4	78	78.8	77.9	76.5
	4Y	67.1	66.1	65.9	66	64.9	58.2	54.4	55.6	58	60.2	62.9	66.7	71.4	75.2	77.6	80	80.4	79.4	78.4
	5Y	69.2	68.3	67.9	68	66.6	58.6	55.3	56.8	59.6	61.7	63.9	67.6	72	75.1	77.1	79.5	80	79	78.1
	6Y	69.9	69.2	68.9	68.8	67.7	60	55.8	56.9	59.4	62.3	65	69.1	74.2	78	79.9	82	82.3	81.6	80.6
Male	Angle	0°	10°	20°	30°	40°	50°	60°	70°	80°	90°	100°	110°	120°	130°	140°	150°	160°	170°	180°
	0M	48.8	48.9	49.7	50.6	49.3	46.1	43.6	43.7	43.7	43.7	44	45.1	47.1	49.2	50.3	51.5	51.6	50.9	51.1
	3M	53.4	53.4	54.3	55.8	55.3	51.1	48.5	49.8	50.4	50.6	51.5	53.4	55.9	58.1	59.6	60.6	60.6	59.7	59.6
	6M	60.1	59.1	59.4	60.2	58.8	53.3	51	52.5	53.2	53.8	55.3	57.9	60.6	63.1	65	66.7	66.6	65.4	64.7
	1Y	65.4	64.1	64.2	64.6	62.5	56.8	53.7	54.9	56.1	56.9	58.5	61.7	65.3	68.7	71.4	74	74.6	73.7	72.6
	2Y	66.8	65.5	65.6	66.2	64.4	58	55.2	56.5	58.6	60	62.1	65.6	69.5	73	75.7	77.8	78.6	77.6	76.7
	3Y	68.4	67	66.9	67.3	65.7	57.1	55	56.6	58.5	60.2	62.6	66.7	71.2	74.7	77.6	80.5	81.4	80.6	79.9
	4Y	69.6	68.5	68.4	68.3	66.7	59.9	56.5	57.7	60.1	62.1	64.4	67.7	72.1	76	78.8	81.9	83	82.2	81.4
	5Y	71.1	70.1	69.7	69.6	68.2	60.5	56.7	58	60.5	63	65.6	69.5	74.4	78.2	80.6	82.9	83.8	83.1	82.2
	6Y	71.4	70.6	70.4	70.4	68.8	61.2	57.7	58.7	61.2	63.8	66.6	70.8	75.5	79.6	82.1	85	85.9	85.2	84.7

Calculated values are rounded off to one decimal place.

DS plane, dorsum sellae plane; HoVA, horizontal vector analysis; 0M, 0 month to 2 months; 3M, 3 to 5 months; 6M, 6 to 11 months; 1Y, 12 to 23 months; 2Y, 24 to 35 months; 3Y, 36 to 47 months; 4Y, 48 to 59 months; 5Y, 60 to 71 months; 6Y, 72 to 83 months.

Table 6 Measurement results of the standard deviation of the DS plane using HoVA

Female	Angle	0°	10°	20°	30°	40°	50°	60°	70°	80°	90°	100°	110°	120°	130°	140°	150°	160°	170°	180°
	0M	2.5	2.4	2.5	2.4	2.4	2.4	2.5	2.4	2.7	2.7	2.6	2.5	2.9	3.3	4.1	4.4	4.6	4.8	5.1
	3M	3.3	3.2	2.9	2.6	2.2	2.5	2.8	2.9	3.1	3.4	3.7	3.8	4.1	4.6	5	5.6	6	5.5	5.3
	6M	3.1	3.1	3.1	2.6	2.3	3	2.7	2.9	3.5	3.7	3.6	3.5	3.4	3.3	3.2	3.2	3.7	4	4.4
	1Y	3.3	3.4	3.2	2.7	2.5	3.8	33.6	3.1	3.5	3.6	3.3	3.2	3	2.7	2.8	3.3	4.1	4.7	4.8
	2Y	3.3	3.3	3.1	2.4	1.8	2.9	2.3	2.4	2.8	3.1	2.8	2.8	2.5	2.8	2.9	2.9	3.4	3.9	4.5
	3Y	3.4	3.4	3.5	3.2	2.6	3.3	2.4	2.3	3	3.7	3.9	4.1	3.6	3.6	3.6	3.7	4.1	4.7	5
	4Y	3.1	3	2.9	2.4	2	3.8	2.8	2.5	2.5	2.8	3.1	3.1	2.6	2.7	2.6	2.5	2.7	3.2	3.3
	5Y	2.9	3	2.9	2.8	2.7	3.2	3	2.8	3	3.2	3.6	3.4	3.2	3.5	3.9	3.8	3.9	3.9	4
	6Y	3.9	3.9	3.6	2.5	1.8	2.9	2.3	2.3	2.6	2.6	2.9	3.1	2.8	2.4	2.6	2.8	3.5	4.2	4.9
Male	Angle	0°	10°	20°	30°	40°	50°	60°	70°	80°	90°	100°	110°	120°	130°	140°	150°	160°	170°	180°
	0M	3.8	4	49.7	3.8	3.5	3.6	3.8	4.1	4.5	4.7	4.7	4.8	5.1	5.4	5.5	5.7	5.8	5.7	5.7
	3M	3.9	4.2	54.3	4.1	3.8	3.8	3.5	3.6	4	3.8	3.3	3.5	3.5	3.7	4.3	4.8	5.5	6	6.1
	6M	4.1	4.2	59.4	3.4	3	3.1	3.3	3.3	3.3	3.6	3.7	3.6	3.5	3.1	3.3	3.4	4	4.4	4.2
	1Y	3.7	3.7	64.2	3.2	2.6	3.2	3.1	3.1	3.4	3.4	3.6	3.7	3.4	3.3	3.6	4	5	5.9	6.1
	2Y	3.8	3.8	65.6	2.7	2.4	3.3	3.1	2.7	3	3.6	3.8	3.8	3.7	3.8	3.9	4	4.9	6	6.3
	3Y	3.2	2.9	66.9	2.4	2.2	3.1	2.8	2.5	2.5	2.7	2.7	2.5	2.6	2.5	2.5	3	4	5	5.4
	4Y	2.5	2.5	68.4	1.7	1.5	3.1	2.9	2.5	2.8	3.4	3.6	3.3	2.8	2.7	2.9	3.3	4	4.7	5.2
	5Y	3.5	3.4	69.7	2.7	2.3	2.5	2.1	2	1.8	1.9	2.1	2.2	2	2.1	2.3	2.5	3	3.8	4.2
	6Y	2.7	2.8	70.4	2.4	1.9	2.6	2.6	2.5	2.5	2.3	2.2	2.3	2.1	2.3	2.7	2.9	3.4	3.7	4.1

Calculated values are rounded off to one decimal place.

DS plane, dorsum sellae plane; HoVA, horizontal vector analysis; 0M, 0 month to 2 months; 3M, 3 to 5 months; 6M, 6 to 11 months; 1Y, 12 to 23 months; 2Y, 24 to 35 months; 3Y, 36 to 47 months; 4Y, 48 to 59 months; 5Y, 60 to 71 months; 6Y, 72 to 83 months.

charts of the mean values obtained using HoVA. The male HoVA values were several millimeters greater than those of the female participants in each age group. Cranial growth was rapid in the first 2 years (especially the first 6 months) of life; afterwards, the growth rate became evidently slower in both sexes and both planes. The growth rate reached a plateau at around 50° earlier than it did at approximately 0° and 180°.

Table 7 Measurement results of the mean of the Max plane using HoVA

Female	Angle	0°	10°	20°	30°	40°	50°	60°	70°	80°	90°	100°	110°	120°	130°	140°	150°	160°	170°	180°
	0M	51.5	51.4	51.5	51	49.9	49.3	48.3	47.5	47.8	48.6	49.3	50	51.3	53.2	55.9	58.3	60	61.5	62
	3M	61.4	61.5	61.8	61.3	59.9	58.6	57.3	57.5	58.2	58.8	59	59.5	60.3	61.3	62.7	64	65	66	66.2
	6M	66.5	66.3	66.6	65.4	63.6	61.6	59.5	59.2	59.9	60.9	62.1	63.3	64.9	67.1	70	73.1	75.4	77	77
	1Y	70.9	70.6	70.7	69.2	67.1	64.6	62.1	61.7	62.8	64.2	65.6	66.9	68.5	70.6	73.6	76.5	78.6	79.9	79.6
	2Y	73.5	73.2	73.1	71.3	69	66.2	63.4	62.8	64.1	65.9	68	69.6	71.3	73.6	77.2	80.9	83.3	85.1	84.8
	3Y	74.3	74	73.9	71.9	69.4	66.6	64	63.3	64.7	66.8	69.1	70.9	72.9	75.5	79.1	82.9	85.8	87.8	87.4
	4Y	73.1	72.6	72.4	71	69	66.9	64.9	64.2	65.6	67.9	70.2	72.2	74.2	76.8	80.3	84	86.9	88.5	88
	5Y	75	74.8	74.8	72.9	70.5	68	65.9	65.2	66.6	68.9	71.3	73.2	74.9	77	80.2	83.8	86.6	88.2	87.8
	6Y	74.7	74.3	74.3	72.8	70.8	68.5	66.6	65.6	66.8	69	71.6	74	76.2	78.5	81.8	85.6	88.4	90.1	89.8
Male	Angle	0°	10°	20°	30°	40°	50°	60°	70°	80°	90°	100°	110°	120°	130°	140°	150°	160°	170°	180°
	0M	54.6	54.9	55.4	55	53.8	52.9	52.1	51.6	51.8	52.2	52.8	53.3	54.4	56.2	58.7	60.5	62	63.1	63.6
	3M	61.4	61.5	62.3	62.3	61.3	60.1	59.1	59.3	60	60.5	61.2	61.8	62.9	64.1	66	67.3	68.8	70	70
	6M	68.1	68	68.4	67.4	65.6	63.8	62	62.3	63.5	64.4	65.4	66.4	67.8	69.2	71	72.8	73.7	74	73.6
	1Y	72.5	72.2	72.4	71.1	69.1	66.9	64.6	64.4	65.4	66.7	68.3	69.7	71.4	73.8	77	80.1	82.2	83.2	82.9
	2Y	73.2	73	73.4	72.3	70.2	68.2	65.9	65.4	67	68.9	71	72.9	74.6	76.7	79.7	82.8	84.9	86.1	85.3
	3Y	75	74.6	74.4	72.8	70.8	68.5	66.3	65.7	67.1	68.8	71	72.8	74.8	77.3	81	85	87.5	89.3	89.1
	4Y	75.5	75.3	75.3	73.9	71.7	69.4	67.2	66.3	67.4	69.3	71.6	73.8	75.8	78.3	81.9	86.4	89.5	91.3	90.9
	5Y	76.2	76	76.2	74.5	72.2	69.6	67.4	66.4	67.8	70	72.6	75	76.9	79.3	82.5	86.2	89.3	91.2	90.7
	6Y	76.9	76.8	77	75.2	73	70.5	68.4	67.5	68.8	70.9	73.4	76.1	78.5	81.1	84.2	88.2	91.5	92.6	92.9

Calculated values are rounded off to one decimal place.

Max plane, plane with the maximal cranial area above the dorsum sellae plane; HoVA, horizontal vector analysis; 0M, 0 month to 2 months; 3M, 3 to 5 months; 6M, 6 to 11 months; 1Y, 12 to 23 months; 2Y, 24 to 35 months; 3Y, 36 to 47 months; 4Y, 48 to 59 months; 5Y, 60 to 71 months; 6Y, 72 to 83 months.

Table 8 Measurement results of the standard deviation of the Max plane using HoVA

Female	Angle	0°	10°	20°	30°	40°	50°	60°	70°	80°	90°	100°	110°	120°	130°	140°	150°	160°	170°	180°
	0M	4.1	4	3.9	3.9	3.6	3.5	3.3	3.3	3.4	3.4	3.3	3.1	2.9	2.7	2.8	3.7	4.5	5.3	5.3
	3M	4.8	4.7	4.5	4	2.9	2.2	2.2	2.6	2.9	2.8	3	3	2.9	2.7	2.9	3.4	4	4.2	4.2
	6M	3.8	3.8	3.8	3.4	3	2.7	2.6	3	3.5	3.6	3.7	3.6	3.7	3.3	3.1	3.4	4	4.5	4.6
	1Y	3.9	3.9	3.9	3.6	3.3	3.1	3	3.2	3.3	3.3	3.2	2.9	2.7	2.5	2.8	3.7	4.7	5.7	5.9
	2Y	3.6	3.6	3.6	3.1	2.6	2.3	2.4	2.6	2.7	2.6	2.4	2.3	2.4	2.3	2.6	3.1	3.7	4.4	4.5
	3Y	4.7	4.9	4.8	4.3	3.8	3.2	2.8	2.7	2.8	3	3.3	3.5	3.5	3.5	3.7	4.3	4.9	5.8	5.9
	4Y	3.6	3.5	3.2	2.6	2.3	2.2	2.3	2.3	2.4	2.3	2.4	2.5	2.5	2.5	2.8	3.2	3.6	4.1	4.4
	5Y	3.1	3.1	3	2.8	2.8	2.8	2.5	2.7	2.5	2.3	2.4	2.6	2.8	3	3.3	4.2	4.9	5.5	5.2
	6Y	4.4	4.2	4	3.6	3.3	2.7	2.6	2.8	2.5	2.5	2.5	2.6	2.9	2.9	3.2	3.7	4.5	5.6	6
Male	Angle	0°	10°	20°	30°	40°	50°	60°	70°	80°	90°	100°	110°	120°	130°	140°	150°	160°	170°	180°
	0M	5.2	5.3	5.3	5.2	5	4.9	4.7	5	5.2	5.3	5.1	4.7	4.3	4	3.8	4.3	4.8	5.2	5.2
	3M	5	5.1	5	4.9	4.2	3.8	3.5	3.4	3.5	3.2	3	3	3.2	3.6	4.5	6	6.7	7.4	7.2
	6M	5.7	5.7	5.6	5.3	4.8	4.3	3.7	3.8	3.9	3.8	3.6	3.2	3	2.8	3	3.7	4.8	5.7	5.8
	1Y	5.1	5.1	5	4.6	4	3.5	3.2	3.4	3.7	3.7	3.7	3.5	3.4	3.4	3.8	4.7	6	7.1	7.2
	2Y	4	3.9	3.7	3.4	2.9	2.5	2.3	2.5	3	3.3	3.5	3.5	3.6	3.4	3.5	4.1	5.3	6.4	6.7
	3Y	4.3	4.2	4	3.5	3.2	2.7	2.6	2.8	2.9	2.8	2.9	2.9	3	3.1	3.3	4.6	5.4	6.6	7.1
	4Y	3.1	3	2.9	2.5	2.1	2.2	2.3	2.3	2.5	2.7	2.8	2.7	2.7	2.4	2.7	3.3	4.2	5.4	5.5
	5Y	4.1	4.2	4.3	3.9	3.4	2.6	2.1	1.9	2	2.2	2.2	2.3	2.3	2.6	2.7	3	3.7	4.6	4.8
	6Y	3.5	3.8	3.9	3.6	3.1	2.6	2.3	2.5	2.7	2.6	2.6	2.3	2.2	2.1	2.6	3.2	4.2	5.7	5.6

Calculated values are rounded off to one decimal place.

Max plane, plane with the maximal cranial area above the dorsum sellae plane; HoVA, horizontal vector analysis; 0M, 0 month to 2 months; 3M, 3 to 5 months; 6M, 6 to 11 months; 1Y, 12 to 23 months; 2Y, 24 to 35 months; 3Y, 36 to 47 months; 4Y, 48 to 59 months; 5Y, 60 to 71 months; 6Y, 72 to 83 months.

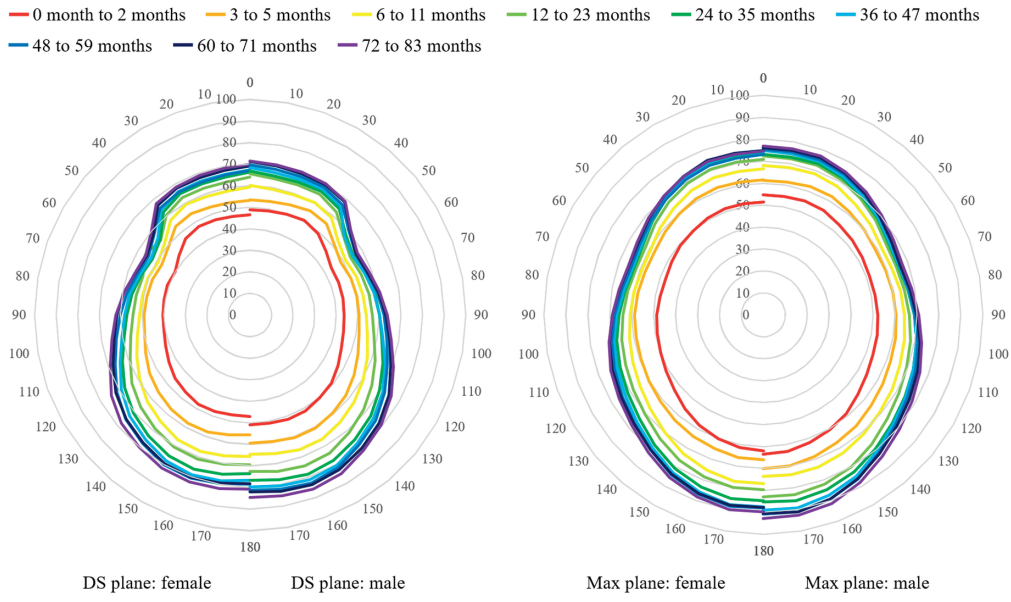

Fig. 6 Horizontal vector analysis radar charts of mean values. DS plane, dorsum sellae plane; Max plane, plane with the maximal cranial area above the DS plane.

Discussion

This study demonstrated that HoVA is a reliable method for measuring two different cranial horizontal planes; furthermore, this study established normal values and the cranial silhouette for each age group by sex in Japanese children.

Imai and Tajima measured the normal morphology for each age group at the anterior half of the DS plane in Japanese children and reported the effectiveness of the values for perioperative evaluation in cases requiring fronto-orbital advancement surgery [17]. Thus, we measured the posterior half of the DS plane, for application to other types of surgeries, as well as the entire Max plane.

Once the measurement error for the area of the Max planes was accepted, there were two or more possible planes within the limits, and the adjacent planes havd similar silhouettes. Thus, we considered 30 mm as an appropriate distance between planes for all age groups, despite the distance between the DS and Max planes of 0M subjects being 1 mm larger than that of 6Y subjects.

After determining the inter-rater reliability, we regarded the correlation coefficients between readers to be sufficiently high and judged that the errors between raters were not different from those within a single rater. Subsequently, we decided that a single person (the primary author) could measure the remainder of the cases.

If the tilt from the true OM plane was within ± 3° on the midsagittal plane (a 6° range), the measurement errors were usually minimal. Realistically, the OM plane could be consistently set within this range in clinical practice. Waitzman *et al.* concluded that if the tilt of the horizontal plane was within ± 4° from the true OM plane, the measurement errors were within clinically acceptable limits [19]. Accordingly, our results were similar to theirs. Therefore, we consider that HoVA was also a reliable method for the determination of measurement error.

In this study, the growth rates measured with HoVA for each age group and sex were consistent with those of reports on the growth rate of head circumference [20] and the growth change shown using MSVA [16]. The cranial growth at the 50° radian reached a plateau on HoVA earlier than the other regions; this site is consistent with the origin of the temporalis. We speculate that this result reflects the development of the temporalis coincident with the development of mastication after age 1-2 years [21, 22].

Our previously published surgical case was examined based on this study's data. We performed cranioplasty using multidirectional cranial distraction osteogenesis [23, 24] in a 31-month-old male patient with

scaphocephaly. We compared the preoperative and postoperative cranial shapes using the Max planes of HoVA and MSVA. The patient's cranial shape improved post-surgically and nearly matched the normal shape when he was 52 months (Fig. 7).

We assume that the decision to use the DS plane or Max plane in clinical practice depends on the patient's original cranial shape and/or the planned operative procedure. The DS plane will be used mainly for fronto-orbital advancement while the Max plane is recommended for cases like our representative case. In addition, combining HoVA with MSVA makes it possible to assess the cranial shape accurately using without complex machines or software.

This study had some limitations. First, although we attempted to exclude cases for whom cranial growth was likely affected, selection bias might have occurred because we did subjectively exclude some patients with conditions that have never been demonstrated to have a negative effect on cranial growth. Second, it is relatively difficult to apply our results to children older than 6 years. Third, it is also difficult to generalize our results to other races because our method was established using only Japanese children.

In future studies more data should be collected, especially for patients older than 6 years. Moreover, although we simply applied the HoVA data of the age group to which the patient belonged for our representative case, it may be necessary to adjust the age group upwards or downwards, depending on the realistic target values. In addition, future studies should establish normal cranial values for coronal planes, and the basement plane should be differently established when the creation of the OM plane becomes difficult, such as in plagiocephaly. Similarly, we should consider developing a new versatile measurement tool to simplify manual measurement.

In conclusion, our HoVA proved a reliable method

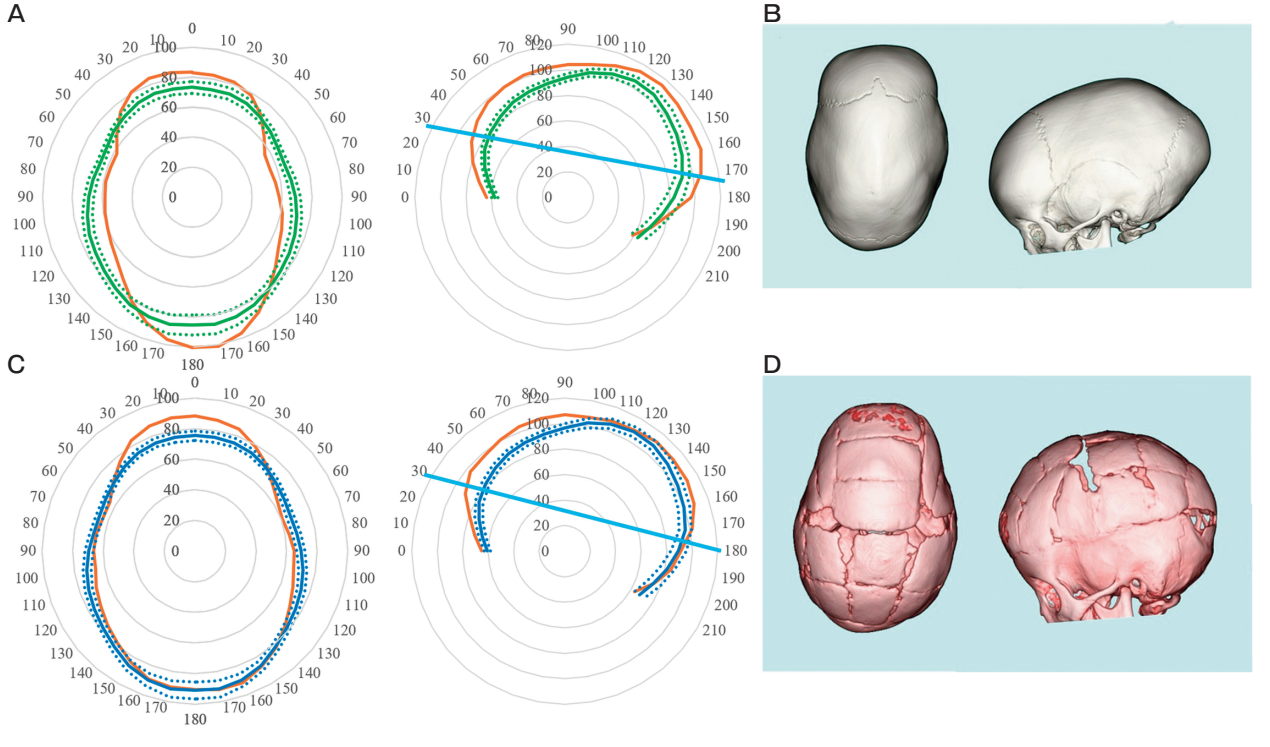

Fig. 7 Clinical application of HoVA. (**A**) Orange lines, preoperative HoVA of the Max plane and MSVA; green lines, normal HoVA and MSVA of the 2Y male group; green dotted-lines, ±1SD lines for normal HoVA and MSVA of the 2Y male group; light blue line, the MAX plane on the midsagittal plane. (**B**) Preoperative 3D CT images. (**C**) Orange lines, postoperative HoVA of the Max plane and MSVA; dark blue lines, normal HoVA and MSVA of the 4Y male group; dark blue dotted-lines, ±1SD lines for normal HoVA and MSVA of the 4Y male group; light blue line, the MAX plane on the midsagittal plane. (**D**) Postoperative 3D CT images. HoVA, horizontal vector analysis; MSVA, midsagittal vector analysis; DS plane, dorsum sellae plane; Max plane, plane with the maximal cranial area superior to the DS plane; 3D CT, three-dimensional computed tomography; 2Y, 24–35 months; 4Y, 48–59 months; SD, standard deviation.

for assessing cranial morphology. We used HoVA to collect the normal cranial values on two different horizontal planes for each age group by sex among Japanese children under 7 years. With HoVA, precise preoperative planning and postoperative follow-up for craniofacial surgery in multiple facilities should be easier to carry out. Future studies should consider more tailored application of HoVA depending on the individual cranial morphology, such the combined use of HoVA with the normal values in the cranial midsagittal plane derived from the previously reported MSVA [15].

Acknowledgments. The authors thank Noriaki Akagi and the radiological technologists of the Department of Radiology at Okayama University Hospital for their technical support in the creation of the database used for this study.

References

1. Koizumi T, Komuro Y, Hashizume K and Yanai A: Cephalic index of Japanese children with normal brain development. J Craniofac Surg (2010) 21: 1434–1437.
2. Likus W, Bajor G, Gruszczynska K, Baron J, Markowski J, Machnikowska-Sokolowska M, Mikla D and Lepich T: Cephalic index in the first three years of life: study of children with normal brain development based on computed tomography. Sci World J (2014) 2014: 502836.
3. Akinbami BO: Measurement of cephalic indices in older children and adolescents of a Nigerian population. Biomed Res Int (2014) 2014: 527473.
4. Ho OA, Saber N, Stephens D, Clausen A, Drake J, Forrest C and Phillips J: Comparing the use of 3D photogrammetry and computed tomography in assessing the severity of single-suture nonsyndromic craniosynostosis. Plast Surg (Oakv) (2017) 25: 78–83.
5. Barbero-Garcia I, Lerma JL, Marques-Mateu A and Miranda P: Low-cost smartphone-based photogrammetry for the analysis of cranial deformation in infants. World Neurosurg (2017) 102: 545–554.
6. Weathers WM, Khechoyan D, Wolfswinkel EM, Mohan K, Nagy A, Bollo RJ, Buchanan EP and Hollier LH Jr: A novel quantitative method for evaluating surgical outcomes in craniosynostosis: pilot analysis for metopic synostosis. Craniomaxillofac Trauma Reconstr (2014) 7: 1–8.
7. Shock LA, Greer S, Sheahan LD, Muzaffar AR and Aldridge K: Consistency of cranial shape measures obtained from laser surface and computed tomography imaging. J Craniofac Surg (2021) 32: 2763–2767.
8. Marcus JR, Domeshek LF, Das R, Marshall S, Nightingale R, Stokes TH and Mukundan S Jr: Objective three-dimensional analysis of cranial morphology. Eplasty (2008) 8: 175–187.
9. Staal FC, Ponniah AJT, Angullia F, Ruff C, Koudstaal MJ and Dunaway D: Describing Crouzon and Pfeiffer syndrome based on principal component analysis. J Craniomaxillofac Surg (2015) 43: 528–536.
10. Kuwahara K, Hikosaka M, Kaneko T, Takamatsu A, Nakajima Y, Ogawa R, Miyazaki O and Nosaka S: Analysis of cranial morphology of healthy infants using homologous modeling. J Craniofac Surg (2019) 30: 33–38.
11. Cho MJ, Hallac RR, Ramesh J, Seaward JR, Hermann NV, Darvann TA, Lipira A and Kane AA: Quantifying normal craniofacial form and baseline craniofacial asymmetry in the pediatric population. Plast Reconstr Surg (2018) 141: 380e–387e.
12. Marcus JR, Domeshek LF, Loyd AM, Schoenleber JM, Das RR, Nightingale RW and Mukundan S Jr: Use of a three-dimensional, normative database of pediatric craniofacial morphology for modern anthropometric analysis. Plast Reconstr Surg (2009) 124: 2076–2084.
13. Saber NR, Phillips J, Looi T, Usmani Z, Burge J, Drake J and Kim PCW: Generation of normative pediatric skull models for use in cranial vault remodeling procedures. Childs Nerv Syst (2012) 28: 405–410.
14. Delye H, Clijmans T, Mommaerts MY, Sloten JV and Goffin J: Creating a normative database of age-specific 3D geometrical data, bone density, and bone thickness of the developing skull: a pilot study. J Neurosurg Pediatr (2015) 16: 687–702.
15. Marcus JR, Stokes TH, Mukundan S and Forrest CR: Quantitative and qualitative assessment of morphology in sagittal synostosis: mid-sagittal vector analysis. J Craniofac Surg (2006) 17: 680–686.
16. Senoo T, Tokuyama E, Yamada K and Kimata Y: Determination of reference values for normal cranial morphology by using mid-sagittal vector analysis in Japanese children. J Plast Reconstr Aesthet Surg (2018) 18: 670–680.
17. Imai K and Tajima S: The growth patterns of normal skull by using CT scans and their clinical applications for preoperative planning and postoperative follow-up in craniofacial surgery. Eur J Plast Surg (1991) 14: 80–84.
18. Katsube M, Rolfe SM, Bortolussi SR, Yamaguchi Y, Richman JM, Yamada S and Vora SR: Analysis of facial skeletal asymmetry during foetal development using μCT imaging. Orthod Craniofac Res (2019) 22: 199–206.
19. Waitzman AA, Ponsick JC, Armstrong DC and Pron GE: Craniofacial skeletal measurements based on computed tomography: Part I. Accuracy and reproducibility. Cleft Palate Craniofac J (1992) 29: 112–117.
20. Kato N, Takimoto H, Yokoyama T, Yokoya S, Tanaka T and Tada H: Updated Japanese growth references for infants and preschool children, based on historical, ethnic and environmental characteristics. Acta Paediatr (2014) 103: e251–e261.
21. Simione M, Loret C, Le Reverend B, Richburg B, Valle MD, Adler M, Moser M and Green JR: Differing structural properties of foods affect the development of mandibular control and muscle coordination in infants and young children. Physiol Behav (2018) 186: 62–72.
22. Keshikawa H, Harada H, Ryuuzaki K and Tamura Y: Electromyographic coordination pattern of masticatory muscles and development of chewing in infants. Jpn J Pediatr Dent (1999) 37: 933–947 (in Japanese).
23. Sugawara Y, Uda H, Sarukawa S and Sunaga A: Multidirectional cranial distraction osteogenesis for the treatment of craniosynostosis. Plast Reconstr Surg (2010) 126: 1691–1698.
24. Gomi A, Sunaga A, Kamochi H, Oguma H and Sugawara Y: Distraction osteogenesis update: introduction of multidirectional cranial distraction osteogenesis. J Korean Neurosurg Soc (2016) 59: 233–241.